UNITED STATES AIR FORCE
RESEARCH LABORATORY

MATHEMATICAL MODELING OF THE
TEMPERATURE RISE IN A THIN CELL CULTURE
EXPOSED TO HIGH FREQUENCY
ELECTROMAGNETIC IRRADIATION

Sherwood W. Samn

HUMAN EFFECTIVENESS DIRECTORATE
DIRECTED ENERGY BIOEFFECTS DIVISION
BIOMECHANISMS AND MODELING BRANCH
2503 GILLINGHAM DR
BROOKS CITY- BASE, TX 78235

June 2003
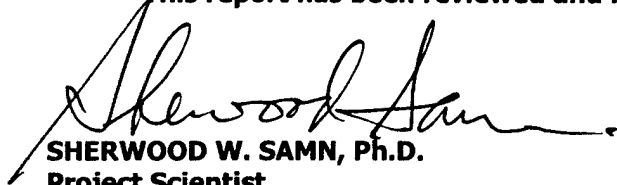
20030829 039

NOTICES

This report is published in the interest of scientific and technical information exchange and does not constitute approval or disapproval of its ideas or findings.

This report is published as received and has not been edited by the publication staff of the Air Force Research Laboratory.

Using Government drawings, specifications, or other data included in this document for any purpose other than Government-related procurement does not in any way obligate the US Government. The fact that the Government formulated or supplied the drawings, specifications, or other data, does not license the holder or any other person or corporation, or convey any rights or permission to manufacture, use, or sell any patented invention that may relate to them.

The Office of Public Affairs has reviewed this paper, and it is releasable to the National Technical Information Service, where it will be available to the general public, including foreign nationals.

This report has been reviewed and is approved for publication.

SHERWOOD W. SAMN, Ph.D.
Project Scientist

RICHARD L. MILLER, Ph.D.
Chief, Directed Energy Bioeffects Division

REPORT DOCUMENTATION PAGE

1. REPORT DATE (DD-MM-YYYY)	2. REPORT TYPE	3. DATES COVERED (From - To)
July 2003	Final	March 2001 – June 2002

4. TITLE AND SUBTITLE
Mathematical Modeling of the Temperature Rise in a Thin Cell Culture Exposed to High Frequency Electromagnetic Irradiation

5a. CONTRACT NUMBER

5b. GRANT NUMBER

5c. PROGRAM ELEMENT NUMBER
62202F

6. AUTHOR(S)
Sherwood Samn

5d. PROJECT NUMBER
7757

5e. TASK NUMBER
B4

5f. WORK UNIT NUMBER
02

7. PERFORMING ORGANIZATION NAME (S) AND ADDRESS (ES)

Human Effectiveness Directorate
Directed Energy Bioeffects Division
Biomechanisms and Modeling Branch
2503 Gillingham Dr.
Brooks City-Base, TX 78235

8. PERFORMING ORGANIZATION REPORT NUMBER

AFRL-HE-BR-TR-2003-0091

9. SPONSORING/MONITORING AGENCY NAMES (S) AND ADDRESS (ES)

10. SPONSOR/MONITOR'S ACRONYM (S)

11. SPONSOR/MONITOR'S REPORT NUMBER(S)

12. DISTRIBUTION / AVAILABILITY STATEMENT
Approved for public release; distribution unlimited.

13. SUPPLEMENTARY NOTES

14. ABSTRACT
This report describes a mathematical model to predict the temperature increase in a thin layer of tissue culture exposed to electromagnetic energy at a frequency of 35 gigahertz (GHz). The goal of the modeling effort was to compare the calculated temperature rise with experimental valves obtained with mouse microphage cell cultures using an infrared camera. The expected temperature increase was calculated using a commercial finite difference time domain code (FDTD). Two problems arise when using FDTD to simulate high frequency electromagnetic radiation of a thin culture to obtain temperature information important to biologists: small time step (necessitating long simulation time) and extrapolation of temperature from specific absorption rates (SARs). In this paper we describe our numerical calculations and compare their results with experimental observations.

15. SUBJECT TERMS
Electromagnetics Propagation Temperature Tissues Diffusion FDTD Specific Absorption Rates

16. SECURITY CLASSIFICATION OF:			17. LIMITATION OF ABSTRACT	18. NUMBER OF PAGES	19a. NAME OF RESPONSIBLE PERSON
a. REPORT	**b. ABSTRACT**	**c. THIS PAGE**			Dr. Sherwood Samn
U	U	U	UL	19	19b. TELEPHONE NUMBER (include area code) (210) 536-5708

Mathematical Modeling of the Temperature Rise in a Thin Cell Culture Exposed to High Frequency Electromagnetic Irradiation

1   Introduction

This report describes a mathematical model to predict the temperature increase in a thin layer of tissue culture exposed to RF energy. This effort is motivated by an experiment conducted by Dr. Nancy Millenbaugh in the Air Force Research Laboratory at Brooks City Base, Texas. To put this mathematical model in the proper perspective, we will describe briefly the biology involved. Heat stroke (sudden fall in arterial blood pressure) can occur under severe hyperthermia, leading possibly to circulatory shock (tissue hypo perfusion). The exact mechanism is still in question. Research suggests that the loss of vasoconstrictor tone and peripheral pooling of blood may be involved in heat-induced circulatory shock. Similar phenomena were observed when heat stress is replaced by millimeter wave (MMW) heating. (The MMW band is from 30 to 300 Hz, corresponding to a wavelength of 10 mm to 1 mm.) However, Freni, et al. [4] suggest that environmental heating and MMW heating are not the same. For one thing, core temperatures under MMW stress do not rise as much as that under environmental heat stress, when circulatory failure begins to occur. For another, MMW exposure can produce larger and more rapid increase in subcutaneous temperature than environmental heating. They suggest that cutaneous thermoreceptor may be responsible for the initiation of circulatory failure during such extreme peripheral heating. For the human body, most of the MMW absorption is in the region of the cutaneous thermal receptors (0.1 mm - 1.0 mm) [5].

To discover possible mechanisms involved in MMW-heating in biological entities, an experiment at Brooks has been conducted to expose cells growing in culture flask by 35 GHz MMW. By submitting the exposed cells for differential gene expression analysis, the researchers hope to find clues to mechanisms underlying MMW-heating.

2   Some Experimental Results

The flask containing the cell culture is shown in Figure 1. A transmitter generating a 35 GHz plane wave is coming from the bottom of the flask and is polarized along its long axis. Using an infrared camera, the temperature in the cell culture can be monitored and captured. An example of the temperature excursion in a cell culture is shown in Figure 2. Another example is shown in Figure 3. However, here a jelatin-like substance (whose heating characteristics

1

are expected to be similar to that of the actual targeted cell culture) is used instead. Figure 4 shows the temperature rise in the same but at two selected cross-sections of the flask. Researchers would like to sample cells for later genetic analysis at locations where the temperature rise is insignificant in order to minimize temperature effects. This would afford them a better chance of discovering possible non-thermal effects of EM radiation. The question is therefore where is the best place to sample the cells? The question is not easy to answer because the observed temperature excursions seem to be sensitive to the experimental setup as the observed temperature excursions are often different from "run" to "run". This is especially true in the earlier experiments (shown, for example, in Figure 2). This could be due a small change in the flask position in the radiation field or in other unknown factors.
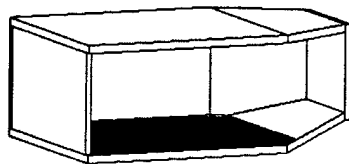

Figure 1: Cut-away flask with cell culture

The goal of the mathematical modeling effort described here is to try to understand what has been observed experimentally. In particular, what temperature excursions are to be expected in the cell culture or its jelatin-like simulant, if the flask is indeed incident by a (35 GHz) plane wave orthogonally. Our approach is to model the experimental setup mathematically. We first calculate the specific absorption rate (SAR) and then use it in turn to calculate the temperature excursion in the cell culture or its jelatin-like simulant. (For simplicity, we will not distinguish between cell culture and its jelatin-like simulant in the following.)
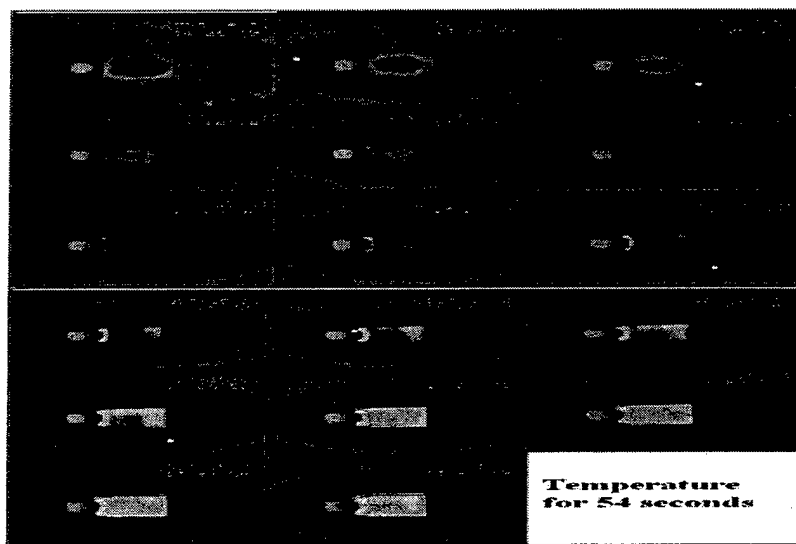
Figure 2: Temperature Excursion at approximately 4-second intervals. Black is "cold" and white is "hot".
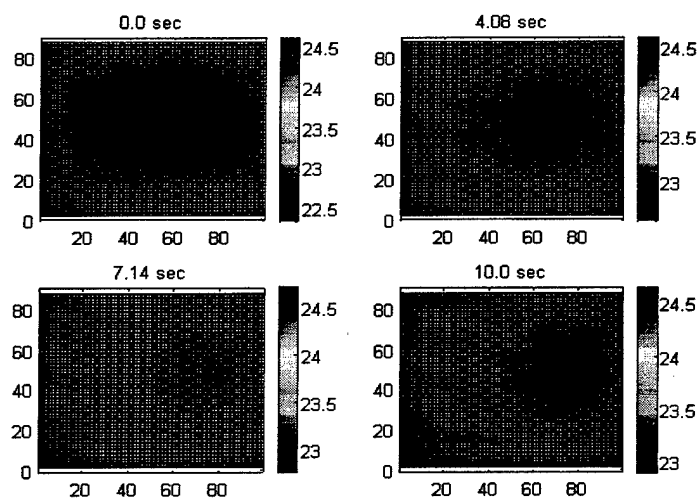

Figure 3: Temperature Excursion at approximately 3.5-seconds intervals in jelatin-like substance. Black is "cold" and white is "hot".
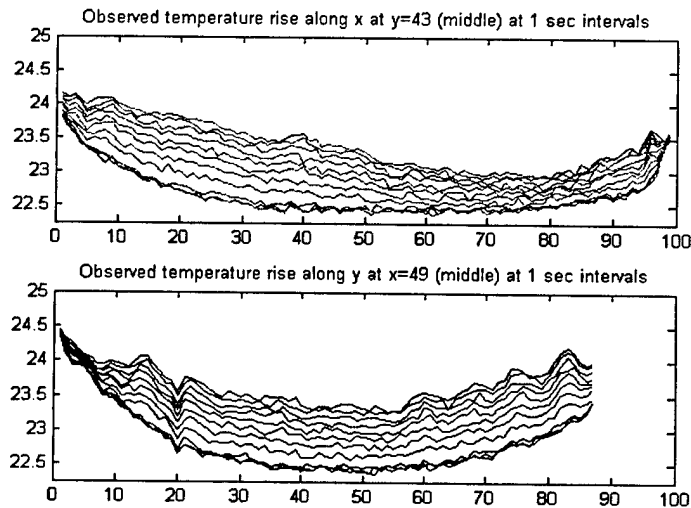
Figure 4: Temperature rise in a jelatin-like substance in selected cross-sections.

3 SAR Calculation

Both the thinness of the cell layer and the high frequency of the incident wave require us to use small spatial resolution ($\Delta x = 150\text{E-}06$ m). This in turn requires us to use very small time steps (approximately 290 fs). To simplify the calculation here and that of the temperature later on, we model the cell culture as being housed in a shallow rectangular flask (Fig 5).
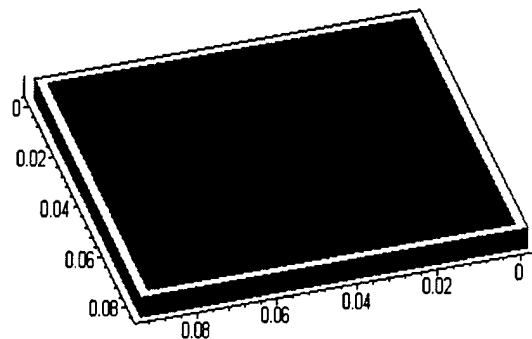

Figure 5: Cell culture in a shallow flask.

We used a commercial finite difference time domain code (XFDTD) to calculate the SAR in the cell culture when it is incident by a 35 GHz plane wave with an amplitude of 86 V/m. The above mentioned spatial resolution results in approximately 14 million Yee cells (Nx x Ny x Nz = 651 x 593 x 36). Fortunately, steady state was achieved in a relatively short time (approximately 0.4 ns, or 1,400 time steps).

The electric parameters used for the flask and the cell culture are shown in Table 1. The average SAR (W/m^3), denoted henceforth by S_V, at a point $\mathbf{r}$ in the flask or in the cell culture is calculated using the formula

$$S_V(\mathbf{r}) = \sigma(\mathbf{r}) \, \|\mathbf{E}(\mathbf{r})\|_{\text{rms}}^2 \tag{1}$$

where $\|\mathbf{E}(\mathbf{r})\|_{\text{rms}}$ is the root mean square value of the electric field (V/m) and $\sigma(\mathbf{r})$ the conductivity (S/m) at the point $\mathbf{r}$. Typical S_V values are shown in Figures 6-7. Figure 6 shows the values of S_V in a layer that includes both the flask and the cell culture. Figure 7 only shows those in the cell culture. It is seen that the highest S_V values tend to be in the interface between the two media.

In most EM dosimetry studies the estimation of S_V is the endpoint. However, for our investigation here, this is only the beginning, as we are interested in knowing the temperature distribution throughout the cell culture beyond the initial exposure. (It is well-known that the initial temperature, for example, during the first few nanoseconds, is directly related to the average SAR.)
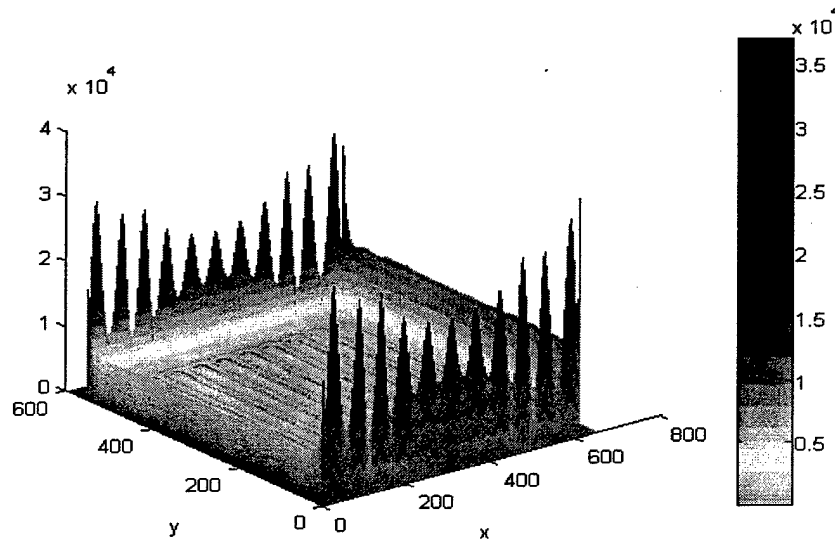

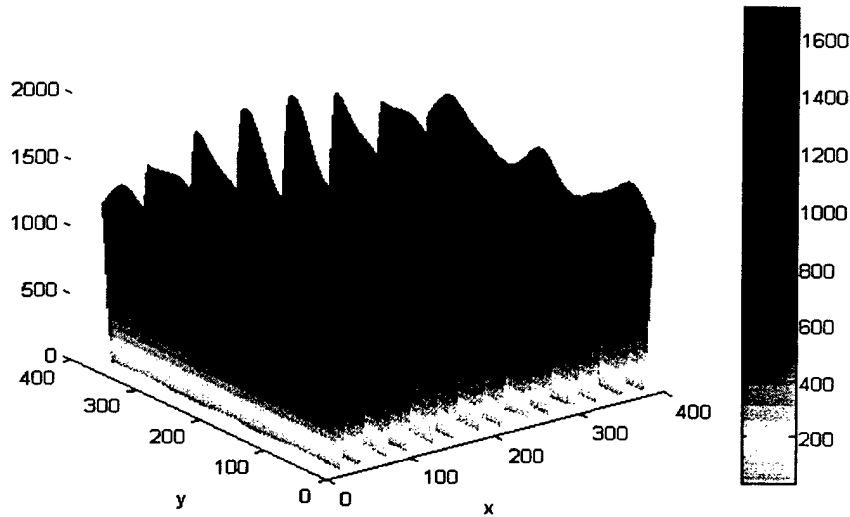Figure 6: Typical SAR in a layer including the flask and the cell culture.

Figure 7: Typical SAR in a layer inside the cell culture only.

4 Temperature Rise Calculation

4.1 3D Diffusion Equation

To calculate the temperature rise, we start with the general 3D heat conduction equation

$$-\nabla \cdot \vec{q} + Q(x,y,z,t) = \rho c_p \frac{\partial T}{\partial t}, \tag{2}$$

$$\vec{q}(x,y,z,t) = -k\nabla T(x,y,z,t) \tag{3}$$

Or, simply,

$$\frac{1}{\alpha}\frac{\partial T}{\partial t} = \nabla^2 T + \frac{1}{k}Q$$

Here $\vec{q} = (q_1, q_2, q_3)$ is the heat flux, wherein each component q_i ($i = 1, 2, 3$) is measured in W/m^2, k is the thermal conductivity (W/m/K), ρ the density (kg/m^2), and c_p the specific heat (J/K/kg). The parameter α is the thermal diffusivity (m^2/s) and is defined by

$$\alpha = \frac{k}{\rho c_p}$$

Finally, Q is the heat source (W/m^3) for the problem.

6

4.2 The 3D Code

The 3D code we used is a modified version of a more general diffusion code obtained from J. Zhang and J. J. Zhao at the University of Kentucky [25]. They use it to solve a special 3D microscale heat transport problem described by the equations (assuming the scale in the z-direction is small in the order of $0.1\,\mu m$),

$$-\nabla \cdot \vec{q} + Q = \rho c_p \frac{\partial T}{\partial t}, \tag{4}$$

$$q_1(x,y,z,t) = -kT_x(x,y,z,t), \tag{5}$$

$$q_2(x,y,z,t) = -kT_y(x,y,z,t), \tag{6}$$

$$q_3(x,y,z,t+\tau_q) = -kT_z(x,y,z,t+\tau_T) \tag{7}$$

where Q a heat source, which in our case is $\sigma \mid \mathbf{E} \mid^2$.

The only differences between Equation (3), the Fourier's Law of heat conduction, and Equation (7) are the time delays τ_q and τ_T. The reason for these time delays (also called relaxation times) is basically to account for the finite speed of heat propagation [18]. As the relaxation times are related to the reciprocals of speeds of heat propagation, the classical model, corresponding to the case in which the "relaxation" times τ_q and τ_T vanish, implies an infinite speed of heat propagation. The insistent of finite propagation speed is especially important in microscale heating, though it may be important in our case also.

Equations (5-7) are clearly related to the dual-phase-lag model of Tzou [18]:

$$\vec{q}(x,y,z,t+\tau_q) = -k\nabla T(x,y,z,t+\tau_T) \tag{8}$$

which in turn is related to many existing microscale heat transfer. When τ_T vanishes in the dual-phase-lag model, Equation (8), one basically gets the well-known Cattaneo and Vernotte (CV) equation [2, 20]

$$\vec{q} + \tau_q \frac{\partial \vec{q}}{\partial t} = -k\nabla T \tag{9}$$

which together with Equation (4) leads to the hyperbolic heat conduction equation

$$\frac{\partial T}{\partial t} + \tau \frac{\partial^2 T}{\partial t^2} = \alpha \nabla^2 T$$

This equation is also known as the thermal wave model or the telegraph equation [9]. There are some experimental observations [14, 10] that resemble hyperbolic heat conduction in living cells as well, although the basic mechanism is still controversial [22].

In this study, we have restricted ourselves to the simple case in which $\tau_q = 0$ and $\tau_T = 0$, and the possibility and the significance of hyperbolic heating in high frequency irradiation will be investigated in the future.

The code uses the Crank-Nicholson method to discretize the differential equation. To solve the resulting large discrete system efficiently, the code uses a

preconditioned conjugate gradient method. The preconditioner uses the incomplete Cholesky factorization of the system matrix which is positive definite and symmetric. All of these computations are done using a sparse representation of the system matrix.

4.3 Boundary Conditions

The solution depends on the external boundary conditions as well as internal boundary conditions. When the Dirichlet boundary condition is applied by setting the boundary temperature to the constant external temperature, a steady state is achieved, as an appropriate amount of heat is continuously being leaked out to balance out the absorbed power. This is contrary to what is observed in the experiment. As the original 3D code handles only Dirichlet boundary conditions, we are led to implement a more realistic mixed ("radiation") boundary condition [1, Carslaw and Jaeger] of the form

$$k\frac{\partial T}{\partial n} + h(T - T_e) = 0$$

where k is again the (internal) thermal conductivity, h the "external conductivity" (W/m^2/K), and T_e the external temperature.

4.4 Internal Boundary Conditions

Our problem is non-homogenous consisting of the flask and the cell culture. As the original code only treats the homogeneous case, we extended the code to handle simple internal boundary conditions (on the surface separating the flask and the culture cell) of the form

$$T_1 = T_2$$

and

$$k_1 \frac{\partial T_1}{\partial n} = k_2 \frac{\partial T_2}{\partial n}$$

where $\frac{\partial}{\partial n}$ is the differentiation along the normal to the surface separating the flask and the culture cell. These new conditions destroy the symmetry of the system matrix and required us to implement a less efficient sparse matrix solver.

4.5 Source

It is natural as well as tempting to use the instantaneous SAR as the source:

$$Q(x, y, z, t) = \sigma \left\| \mathbf{E}(x, y, z, t) \right\|^2$$

However, it soon becomes clear that this is highly impractical due to the high frequency (35 GHz) involved. If we were to make full use of the instantaneous SAR, we would need to use a time step on the order of a few picoseconds.

This becomes impractical to solve (especially on a PC), since each step involves solving a system of approximately a quarter of a million unknowns, even when we use a moderately refined spatial discretization. The second best choice is therefore to use the time-averaged SAR defined in Equation (1) as the source, i.e.,

$$Q(x, y, z, t) = S_V(x, y, z)$$

4.6 Parameters

Since it is difficult to find the exact heat-related parameter values for our problem, we have "averaged" parameter values extracted from the following sources:

- Lu, et al. [12] have parameters for different human tissues (eye, bone, brain, skin and CSF) at 1 GHz. The values (averaged) are ($e_r = 49.76, \sigma = 1.24$ S/m, and $k = 0.48$ W/m-K)

- Van Leeuwen, et al [19] have the following parameters (averaged) for brain tissues: $e_r = 54.89, \sigma = 1.22$ S/m, $k = 0.48$ W/m-K, $c_p = 3529$ J/kg-K, and $\rho = 1014$ kg/m.

- Wainwright [21] has parameters for various human tissues. The averaged values are: $\rho = 1125$ kg/m^3, $k = 0.42$ W/m-K , $c_p = 3210$ J/kg-K,

- Hirata, et al. [6] have values for human eye tissues. The averaged values are: $c_p = 3838$ J/kg-K, and $k = 0.54$ W/m-K

- Hurt [7] recommends the following electric parameters at 35 GHz: $\sigma = 60$S/m, and $e_r = 22$ for cell culture and $\sigma = 0$ S/m, and $e_r r = 2.4$ for the flask.

- For the possible flask's electric conductivity, Stratton [17] has $\sigma = 1.0E - 08$ S/m for celluloid.

- From [8] we have the following heat parameters for flask (semiconductor), $c_p = 250$ J/kg-K and $\rho = 5000$ kg/m^3

- From [16] we have heat parameters for glass: $k = 0.836$ W/m-K

- From Internet Web Site MatWeb.com, we have, for Polystyrene, $\rho = 1050$ kg/m^3, $c_p = 1800$ J/kg-K, and $k = 0.14$ W/m-K

The initial values of the model parameters are summarized Table 1.

9

Table 1. Model Parameters

Parameters	Cell	Flask
e_r	22	2.4
σ (S/m)	60	5.74E-04
k (W/m-K)	0.48	0.14
ρ (kg/m^3)	1070	1050
c_p (J/kg-K)	3526	1800
Derived Parameters		
α (m^2/s)	1.27E-07	7.4E-08
$\frac{1}{k}$ (m-K/W)	2.085	7.14

4.7 Initial Conditions

Using the parameters in Table 1 and an assumed constant initial (room) tem-
perature throughout, we were, unfortunately, unable to produce temperature
profiles that match (qualitatively) the experimental observations. The same is
true when we experiment with (many) different sets of parameter values. This
led us to think that the assumption of constant initial temperature may not be
valid. Consequently, instead of using a constant initial temperature, we use an
initial temperature profile that is an approximation of the observed (see Figure
8). The difference between the actual and its approximation is shown in Figure
9.

4.8 Final Parameter Adjustments

As we cannot be certain if the parameter values for the jelatin-like substance
used in the experiment of interest (cf. Figures 3 and 4) are similar to that for the
estimated cell culture values shown in Table 1, we allowed ourselves the freedom
to adjust these parameter values to match the experimental results qualitatively.
The most significant change is the thermal conductivity. The numerical results
we will show in the following used a thermal conductivity of 24 (W/m/K) for
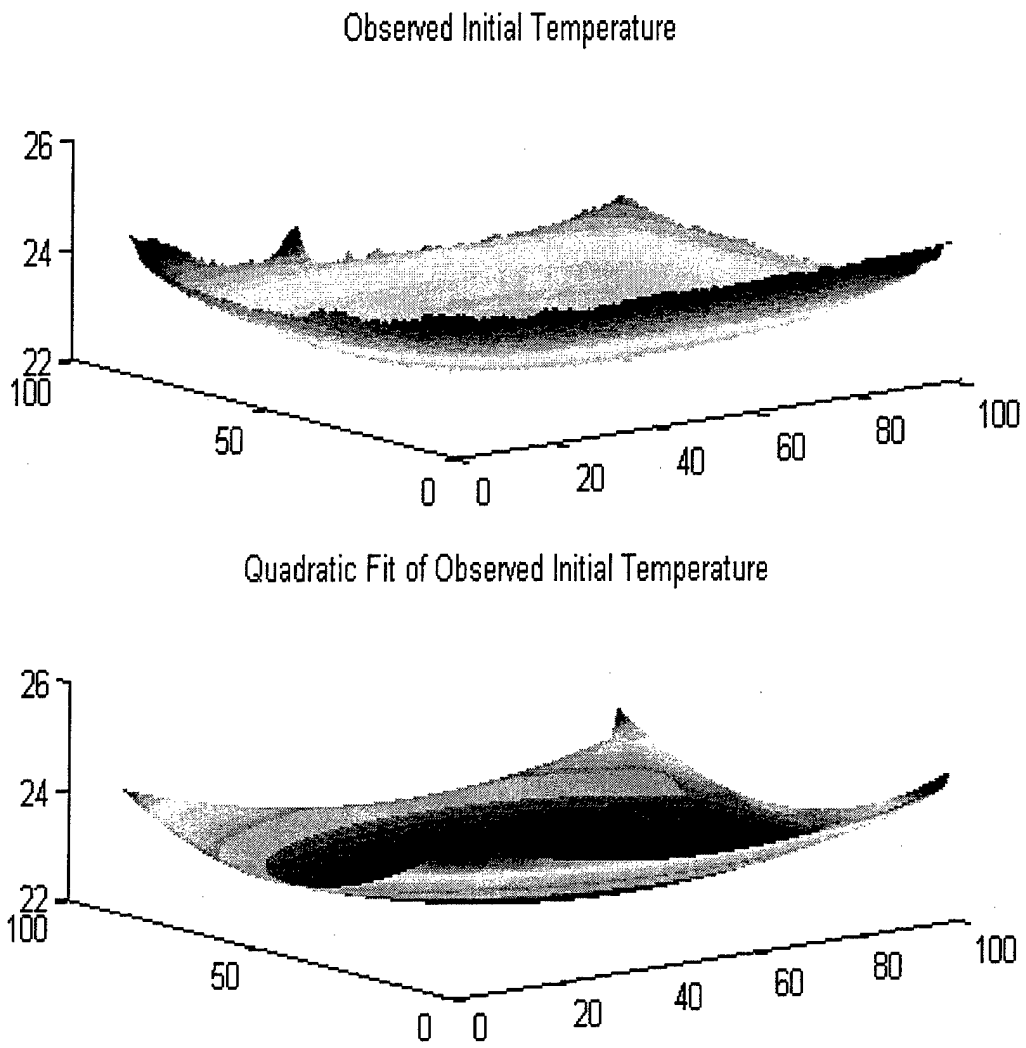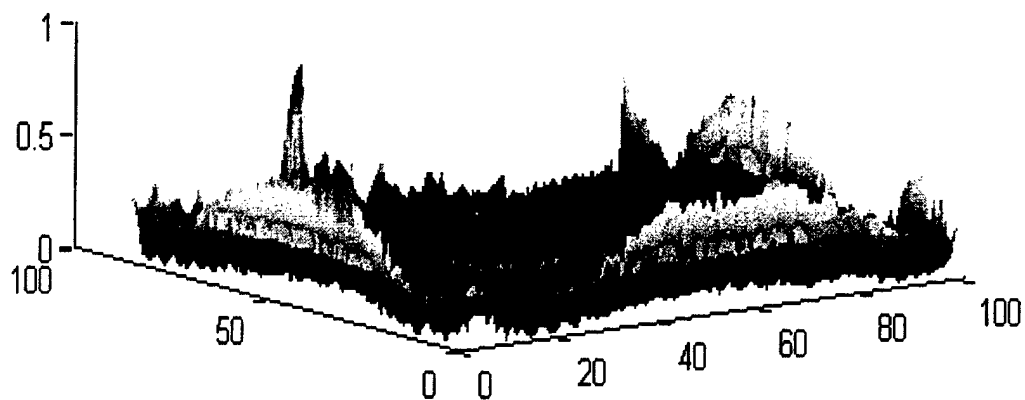the jelatin-like substance instead of 0.48 (W/m/K) estimated for cell cultures
in Table 1.

Observed Initial Temperature

Quadratic Fit of Observed Initial Temperature

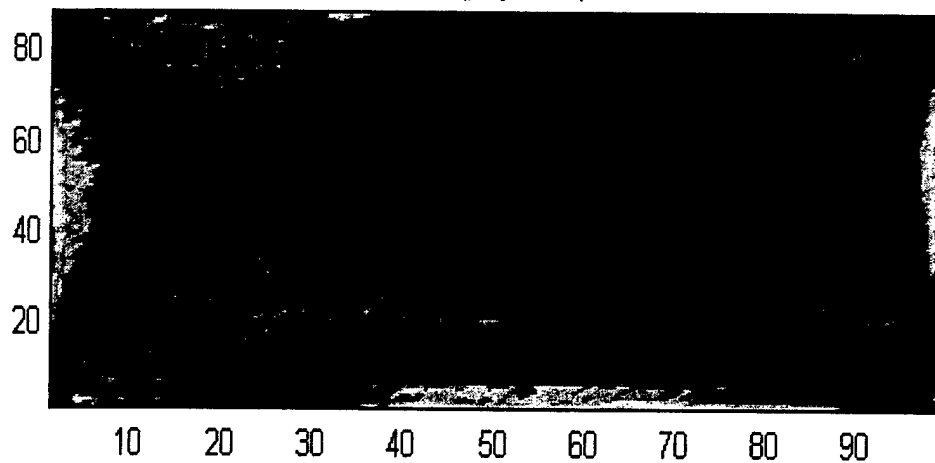Figure 8: Initial temperature rise (at t=0 sec) and the quadratic fit.

Figure 9: Fit error: surface and projected views. Dark is low and bright is high.

5 Simulation Results

Simulation results are shown in Figures 10-13. Figure 10 shows the temperature profiles at different times along a middle x-section (bottom figure) and a middle y-section (top figure). Qualitatively, this compares reasonably well with the experiment results shown in Figure 4. Recall the experiment uses a flask (cf. Figure 1), whereas the simulation uses a rectangular box (cf. Figure 5).

Figure 11 shows the temperature profile in a layer near the top at four different times.

Figures 12 and 13 show two different views of temperature profiles in the entire jelatin-like substance after 10 seconds. Figure 12 is drawn to scale.
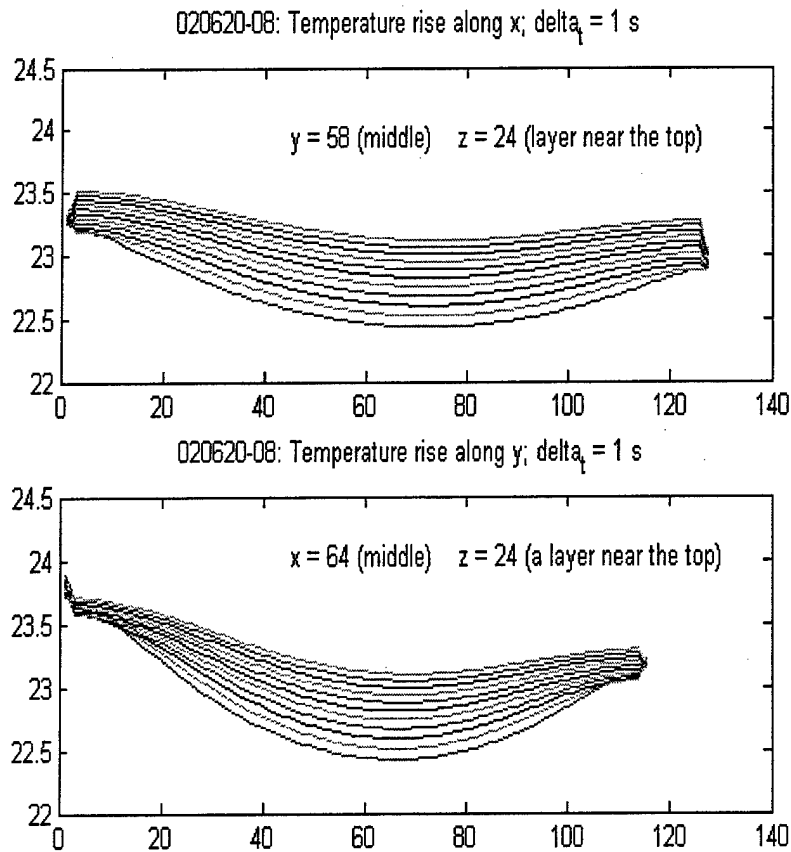

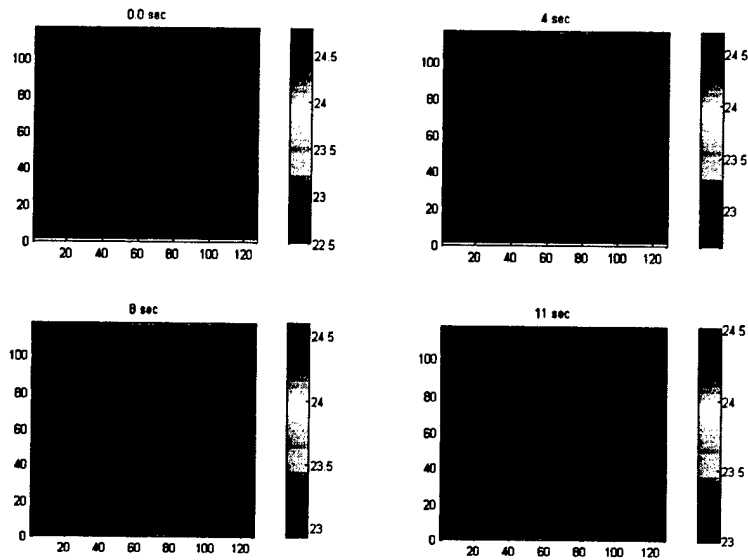Figure 10: Simulated temperature rise in selected cross-sections.

Figure 11: Simulated temperature distribution in a layer near the top (z=24) at 4 different times.
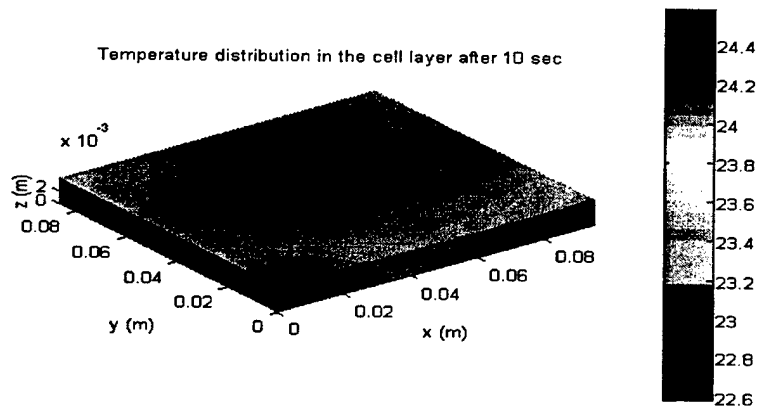

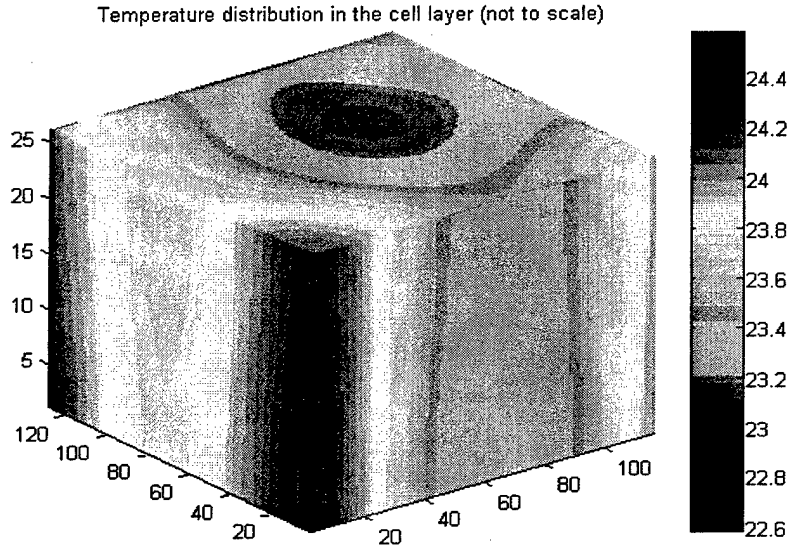Figure 12: Simulated temperature distribution in the whole cell culture after 11 sec.

Figure 13: Simulated temperature distribution in the whole cell culture after 11 sec. (Not to scale.)

6   Conclusion/Discussion

We used a combination of a 3D electromagnetic code and a 3D heat diffusion model to study the temperature rise in a thin layer of jelatin-like substance that is placed in a flask while incident by a 35-GHz electromagnetic plane wave. This is motivated by the need to estimate temperature rise in cell cultures in similar experiments.

We used a finite difference time domain (FDTD) code to solve the electromagnetic portion of the problem. Due to the high frequency involved and the thinness of the cell culture, it took about 30 hours to obtain the steady state SAR on our Sun workstation. A faster code like the VMAX (Monopole Research) has solved a similar problem in about 6 hours on a similar platform.

The 3D heat diffusion model we used is a special case of the Pennes bioheat equation [15]

$$\rho c_p \frac{\partial T}{\partial t} = k\nabla^2 T + c_b (T - T_b) + \sigma \mid \mathbf{E} \mid^2$$

often used to study temperature rise in human exposed to an electromagnetic field. The Pennes bioheat model and other more elaborate models [23] take into

15

account, among other things, the role of blood flow in the tissues. The special case we have here does not have to deal with this aspect.

The 3D diffusion equation solver is normally quite efficient for the simple homogeneous problem, but less so for the inhomogeneous case. In the latter, one has to deal with an internal boundary (here between the flask and the cell culture). Dai and Nassar [3] used a "domain decomposition" method to solve the problem by basically solving two separate problems, one on each domain, and used an iterative method to match up the solution on the common boundary. The method we employed is simpler but did destroy the symmetry and hence the efficiency. When the domain of computation is irregular, then a boundary element type method may be better [13].

There is also a basic question on what the infrared camera is capturing. The color at each point in each picture frame obviously correlates to some temperature. The question is how does a 3D temperature distribution transform to the 2D distribution recorded by the camera? What type of integration does one need to perform on the 3D temperature distribution to obtain the 2D distribution captured by the camera? Or, does the infrared camera only capture only the temperature distribution on the surface?

In a series of papers J. Liu et al. [11] proposed a skin burn model that is different from the traditional Pennes' bioheat equation. It includes thermal waves due to "delay" or inhomogeneity in skin. The model, called the thermal wave model for bioheat transfer(TWBMT), yields results quite different from that using the Pennes's formulation, especially for a "flash fire" situation (high flux heating with extremely short duration). This suggests the traditional heat equation may not be an appropriate model for MMW stress.

The energy equation (2) is valid for rigid bodies only [9]. It is implicitly in the Pennes's bioheat equation also. As most biological organs cannot strictly be considered as rigid bodies, studies using the Pennes' bioheat equation as well as the present study should be re-examined using a more appropriate energy equation.

In the attempt to match the experimental results for jelatin-like substance, we had to increase the values of some parameters to over and above those expected for actual cell cultures. This increase in parameter values allows us to match the temperature increase observed in the experiment. Without this increase in parameter values, i.e. if we had used parameter values documented in the literature for tissues, the temperature increase would have been less.

Finally, as far as matching experimental results is concerned, the initial temperature value in the jelatin-like substance is one of the most crucial components of the calculation. It is still unclear why the temperature is not uniform at the beginning of the experiment.

7   Acknowledgment

References

[1] H. S. Carslaw and J. C. Jaeger, *Conduction of Heat in Solids* Oxford at the Clarendon Press, 1959.

[2] C. Cattaneo, *A Form of Heat Conduction Equation Which Eliminates the Paradox of Instantaneous Propagation.* Compte Rendus, Vol. 247, pp. 431-433, 1958.

[3] W. Dai and R. Nassar, *A Domain Decomposition Method for Solving Three-Dimensional Heat Transport Equations in a Double -layered Thin Fil;m with Microscale Thickness.* Numerical Heat Transfer, Part A, 38:243-255, 2000.

[4] M. R. Frei, K. L. Ryan, R. E. Berger, and J. R. Jauchem, *Sustained 35-GHz Radiofrequency Irradiation Induces Circulatory Failure.* Shock, Vol. 4, No. 4, pp. 289-293, 1995.

[5] O.M.P. Gandhi, *Absorption of Millimeter Waves by Human Beings and Its Bilogical Implications.* IEEE Trans. Microwave Theory and Tech., Vol. MTT-34, No. 2, Feb, 1986.

[6] A. Hirata, S. Matsuyama, and T. Shiozawa, Temperature Rises in the Human Eye Exposed to EM Waves in the Frequency Range 0.6 - 6 GHz. IEEE Trans. Elect. Comp., Vol. 42, No. 4, Nov., 2000.

[7] Oral communication, 2001.

[8] CRC Handbook of Chemistry and Physics, 77th Edition, 1996.

[9] D. D. Joseph and Luigi Preziosi, *Heat Waves.* Reviews of Moern Physics, Vo. 61, pp. 41-73, 1989.

[10] W. Kaminski *Hyperbolic Heat Conduction Equation for Materials With a Nonhomogeneous Inner Structure.* J. of Heat Transfer, Vol. 112, pp. 555-560, 1990.

[11] J. Liu, X. Zhang, C. Wang, W. Lu, and Z. Ren, *Generalized Time Delay Bioheat Equation and Preliminary Analysis on its Wave Nature.* Chinese Science Bulletin, Vol. 42, No. 4, Feb 1997.

[12] Y. Lu, J. Ying, T. K. Tan, and K. Arichandran, *Electromagnetic and Thermal Simulations of 3-D Human Head Model under RF Radiation by Using the FDTD and FD Approaches* IEEE Trans. Magnetcs, Vol. 32, No. 3, May, 1996.

[13] W. Q. Lu, J. Liu, and Y. Zeng, *Simulation of the Thermal Wave Propagation in Bilogical tissues by the Dual Reciprocity Boundary Element Method.* Engineering Analysis with Bounary elements, Vol. 22, pp. 167-174, 1998.

[14] K. Mitra, S. Kumar, A. Vedavarz, and M. K. Moallemi, *Experimental Evidence of Hyperbolic Heat Conduction in Processed Meat.* J. of Heat Transfer, Vol. 117, pp. 569-573, 1995.

[15] H. H. Pennes, *Analysis of Tissue and Arterial Blood in the Resting Human Forearm.* J. Appl. Physiol., Vol. 1, pp. 93-1948.

[16] R. W. Sears and M. W. Zemansky, *University Physics, 3rd Ed.* Addison-Wesley Pub. Co. Inc., 1963;

[17] J. A. Stratton, *Elecctromagnetic Theory.* McGraw-Hill, Inc., 1941.

[18] D. Y. Tzou, *Macro-to Microscale Heat Transfer, The Lagging Behavior* Taylor & Francis, 1997.

[19] G. M. J. Van Leeuwen, J. J. W. Lagendijk, B. J. A. M. Van Leersum, A. P. M. Zwamborn, S. N. Hornsleth, and A. N. T. J. Kotte, *Calculation of Change in Brain Temperatures due to Exposure to a Mobile Phone.* Phys. Med. Biol., Vol. 44, pp. 2367-379, 1999.

[20] P. Vernotte, *Some Possible Complications in the Phenonmena of Thermal Conduction.* Compte Rendus, Vol. 252, pp. 2190-191.

[21] P. Wainwright, *Thermal Effects of Radiation from Cellular Telephones.* Phys. Med. Biol., Vol. 45, pp. 2363-2372, 2000.

[22] L. X. Xu and J. Liu *Discussion of Non-Equilibrium Heat Transfer in Biological Systems.* Advances in Heat and Mass Transfer in Biotechnology, ASME, pp. 13-17, 1998.

[23] L. X. Xu, *New Developments in Bioheat and Mass Transfer Modeling.* Annual Review of Heat Transfer, Vol. 10, pp. 1-23, 1999.

[24] D. Y. Yuan, J. W. Valvano, E. N. Rudie, and L. X. Xu, 2-D Finite Difference Modeling of Microwave Heating in the Prostate. ASME Winter Annual Meeting, 1995.

[25] J. Zhang and J. J. Zhao, *Iterative Solution and Finite Difference Approximations to 3D Microscale Heat Transport Equation.* (Preprint) 2001.